Landmark detection by a rotary laser scanner for autonomous robot navigation in sewer pipes

Matthias Dorn, Matthew Browne and Saeed Shiry Ghidary
GMD-Japan Research Laboratory, Kitakyushu, Japan
E-mail: {matthias.dorn}{matthew.browne}{saeed.shiry}@gmd.gr.jp

Abstract: This paper demonstrates the successful autonomous classification of rotary laser scanner data retrieved by an autonomous robot traversing a sewer pipe system. Rotary laser scanner serve dual purposes of fault detection and navigation. The present aim was to devise a robust landmark detection method for use in the robot's navigation system. A standard feed forward neural network with 6 hidden neurons was trained on the first 15 principle components of the combined amplitudes of the reflected signal and distance values data. The overall system shows a 89% performance for the classification for the validation data as opposed to 79% of a linear neural network. These results demonstrate that the appropriate application of conventional sensor feature extraction, and classification methods may be used to quickly build an effective and computationally efficient landmark detection system for a mobile robot.

Keywords: landmark detection, sewer pipes, rotary laser scanner, autonomous robots, classification task, feed forward neural network, principle components analysis,

1 Introduction

Recent research in service robotics has focused on the development of autonomous sewer inspection robots [1, 2, 3] and automatic fault detection systems [4, 5]. Hertzberg et. al. [6] give an introduction into conventional inspection procedures, its drawbacks and show the role artificial intelligence and information technology approaches can play in offering solutions. With regard to successful applications of innovative sensors to multi sensor fusion in order to detect artefacts in sewer pipes, an approach can be found in [7]. We consider landmark detection for navigation purposes as an important component of introducing autonomous robotic systems for sewer pipe inspection.

In this paper, we present an implementation of autonomous landmark detection on a mobile robot using a mounted rotary laser scanner, feature extraction, and neural network-based classification. As opposed to other common sensors used in robot navigation, e.g. infrared and ultrasound sensors, the rotary laser scanner combines several positive aspects: it is insensitive to common artefacts in data aquisition, optical shades and hues, and redundant signals due to reflection and limited range. Furthermore, the data can be used for multiple purposes: identification of artefacts in the pipe, damage identification and deformation identification.

2 System hardware

The system as shown in fig. 1 is based on the Kurt2 autonomous robotic platform, as introduced by Kirchner et. al. [8]. It was developed by the Fraunhofer Institute for Autonomous intelligent Systems (AiS), Germany, as a first study for autonomous sewer inspection platforms. The control unit is a Pentium III 600 mhz processor, running under the linux operating system, which contains the navigation, data retrieval and processing software. Main sensor for the data retrieval task is a commercially available rotary laser scanner, see table [1] for technical specifications. The main feature of this rotary laser scanner is the fact that it acquires both distance values and amplitudes of the reflected signal. Furthermore, it rotates perpendicular to the direction of motion, acquiring circular scans of the pipe surface. Due to the limited rotation speed of the rotary laser scanner, the travelling velocity of the robot was set low enough to be able to ignore the step size and treat all scans as belonging to the same pipe section, see fig. 2 for a schematic depiction.

All on board-sensors, motors of the robot, rotary laser scanner and control unit are connected with via the CAN bus system, described in [9], [10].

3 Experiments

We have conducted a series of experiments at the experimental site of AiS[1]. The test site consists of a system of standard concrete pipes used in german sewer systems. The robot system was employed into this experimental sewer system for a series of 10 runs consisting of a total of 5 hours running time. For easy

[1] courtesy of: Fraunhofer Institute for Autonomous intelligent Systems, Schloß Birlinghoven, Germany

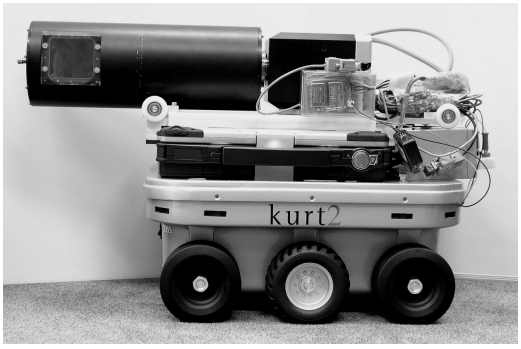

Figure 1: Kurt2 with mounted rotary laser scanner

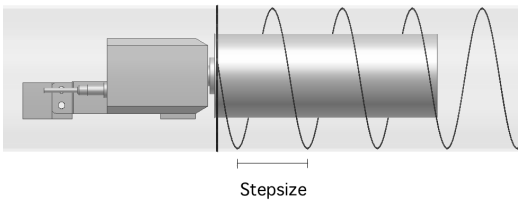

Figure 2: Schematic depiction of step size

access, the pipe system is situated above ground. Fig. 3 shows two views on the experimental site. To the left, the central intersection with manhole is depicted, with an inlet visible. To the right, one of 3 curve sections with manhole can be seen.

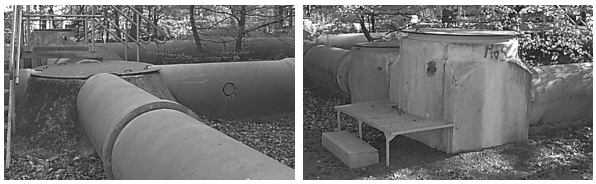

Figure 3: Test site at AiS, Germany: Example of Class 3/6 (Inlet) and Class 5 (pipe intersection & manhole) (left) and Class 4 (curve section & manhole) (right)

4 Data analysis

In a learning phase, reference data is acquired in a test environment. The test environment consists of 6 environmental states. These are defined in table 2: normal section, pipe joints, inlet to the left, curve section with, pipe intersection with manhole and inlet to the right. The goal of analysis is to process the 939 scan samples of a single rotation, categorizing with regard to the presence of different environmental features. We take an unsupervised dimension reduction approach, applying principle components analysis (PCA) for dimensionality reduction, collapsing the signals onto the 15 largest axes of variance. Linear and non-linear classifiers were then optimized for class prediction using PCA scores as input. The final system is implemented online efficiently as projection on a relatively small set of orthogonal basis vectors, followed by neural network simulation.

Table 1: Specification of the rotary laser scanner

Specification	Value
rpm	60−120 rpm.
resolution	720 ppr. (0.5)
accuracy	+/− 1 mm
fast response time	50 kHz max.
emitter	780 nm IR laser diode
optical power	8 mW max.
beam diameter	2.5 mm
beam deviation	0.5 mrad
power	5V, 5A DC and 12V , 2A DC
operating range	0 m to 20 m
output	distance in inches or mm
	amplitudes of the reflected signal

Table 2: Definition and frequency of classes

Class	Description	relevance
1	normal section	21%
2	pipe joints	16%
3	inlet to the left	13%
4	curve section & manhole	15%
5	pipe intersection & manhole	21%
6	inlet to the right	14%

4.1 Preprocessing

The original data consists of 6525 single scans. Each scan yields distance values from the rotary laser scanner to the sewer pipe wall as well as the amplitudes of the reflected signal. Fig. 4 shows an exemplary section of the data set, with amplitudes of the reflected signal to the left and distance values on the right side. The top section displays the data acquired passing a manhole, whereas the anomaly in the lower part can be attributed to an inlet. The large noise visible in amplitudes of the reflected signal can be accounted for due to the nonuniform surface structure of the concrete pipe surface, e.g. mold growth, decay or chipped off parts. On the other hand, distance values display a more coherent picture. The graduation is caused by the eccentricity of the laser from pipe center. We abstained from centring the data with respect to the pipe center due to the non-uniform motion of the robot in the pipe, caused by meandering motion an obstacles such as stone and debris on the ground.

The distance values larger than an arbitrary value of 450 mm for a pipe radius of 300 mm were set arbitrarily to 640 mm. This is valid for the cases when the

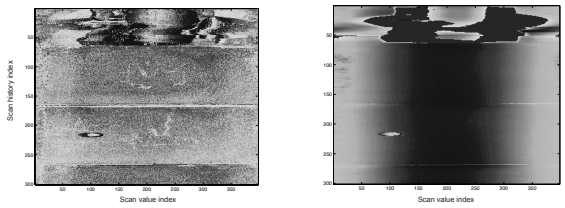

Figure 4: Example scans of acquired data: amplitudes of the reflected signal (left) and distance values (right)

robot passes intersections or manholes and the laser beam is reflected by instead the pipe wall by either the manhole lid or reaches its limit.

Secondly, the data set was classified manually into the 6 most prominent features, see table [2]. Since the feature "normal section" was originally predominant with a relevance of 88%, the validation data set was adjusted to offer approximately evenly distributed classes. Fig. 5 shows examples for each of the classes.

Thirdly, we have created a data set of both the distance values and the amplitudes of the reflected signal and presented it to the PCA schema.

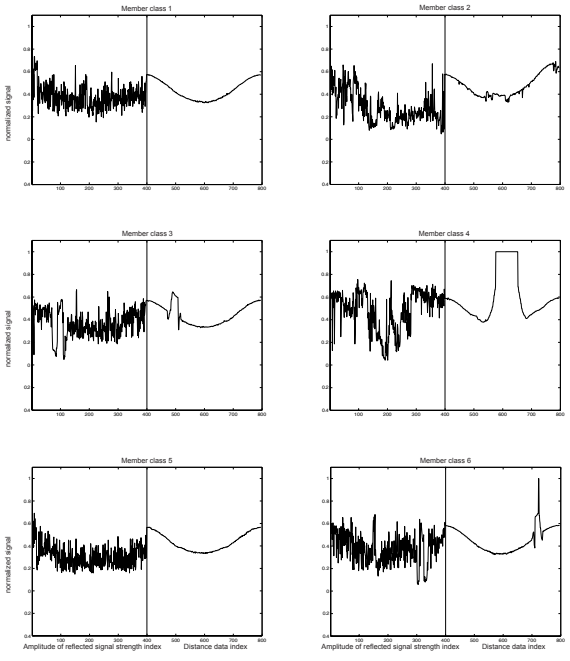

Figure 5: Class members for each class 1 - 6 from top left to lower right: amplitudes of the reflected signal for $[1, 398[$ and distance values for $[399, 796[$

4.2 Principle components analysis

By solving for the eigenvalues and eigenvectors of a matrix, PCA determines an orthogonal linear transformation that maximizes the explained variance in as few variables as possible. It is a widely recognized tool for data dimensionality reduction [11]. In this case the first 15 principal components (PC) λ_i in fig. 6 describe 98% of the explained variance in the data, see fig. 7.

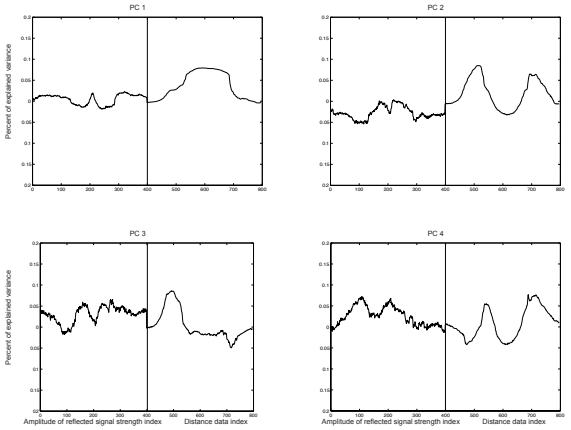

Figure 6: First four PCs λ_{1-4}, contributing to $\lambda_1 = 0.8089, \lambda_2 = 0.1090, \lambda_3 = 0.0278, \lambda_4 = 0.0149$ percentage of the explained variance, amplitudes of the reflected signal for $[1, 398[$ and distance values for $[399, 796[$

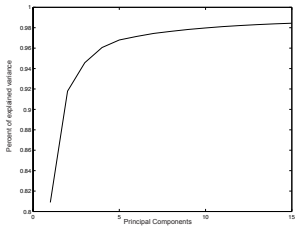

Figure 7: Accumulated explained variance of first 15 PCs:$\sum \lambda_i = 98\%$

4.3 Classifier

We tested linear and non-linear classifier systems. The linear classifier system was implemented using a standard feed-forward methodology, with no hidden neurons, and log-sigmoid transfer functions in the output layer. This effectively implements linear logistic regression, which is appropriate when the desired outputs are class labels rather than variables. The non-linear system was implemented using a similar feed-forward architecture, using 8 neurons in the hidden layer, utilizing hyperbolic tangent sigmoid transfer functions.

In both bases, the first 15 principle components served as input to these feed forward backpropagation networks. The output consisted of the six predicted class probabilities. The training epochs were limited to 50 steps. Model optimization was implemented using the Levenberg-Marquardt [12], [13] backpropagation algorithm.

4.4 Validation Method

We apply cross validation schema for performance measure [14] and make use of its better performance when used with small data sets as opposed to methods such as split-sample validation [15]. In our case, the data is divided 10 times into 90% training and 10% validation subsets. The classifiers are trained and validation 10 times, and the validation performance summed. In the non-linear case the network is trained 9 times, and the performance of the best performing network considered.

5 Results

The non-linear classifier performed significantly better than the linear classifier, with validation performances of 89% and 79%, respectively. The classification in detail for both the linear and nonlinear neural networks are shown in tables 3 and 4. Displayed are absolute figures of the sum of the classification results of the best performing nonlinear neural network of 9 validation runs.

Table 3: Classification of the linear neural network against the validation set, performance: 79%. Shown are absolute values

	Validation						
Model	Class	1	2	3	4	5	6
	1	140	39	9	2	2	22
	2	32	80	5	4	10	4
	3	4	5	92	0	2	0
	4	1	1	0	117	11	0
	5	3	4	0	2	151	0
	6	3	7	0	1	0	84
$\sum$		183	136	106	126	176	110

Table 4: Classification of the nonlinear neural network against the validation set, performance: 89%. Shown are absolute values

	Validation						
Model	Class	1	2	3	4	5	6
	1	161	22	2	0	3	4
	2	14	94	0	1	6	0
	3	4	5	104	0	1	0
	4	1	0	0	124	7	0
	5	2	4	0	1	159	0
	6	1	11	0	0	0	106
$\sum$		183	136	106	126	176	110

In the first column of table 4 we note a false classification of 14 cases, which amounts to 7.6%, where the model yielded a class 2 instead of correct class 1. Fig. 8 shows one example of this false classification. On the other hand for the expected class 2, the model falsely classified 22 cases, which amounts to 16% of all cases. This is shown with an example in fig. 9. Thus, a large proportion of the model errors were in distinguishing normal section and pipe joints. From these figures it can be seen that the input data corresponding to these cases bears a very high similarity. It is likely that these classes may be effectively distinguished by considering the history information, incorporating consecutive scans for landmark detection.

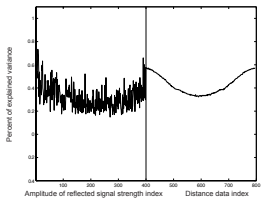

Figure 8: Example of falsely classified scans: identified class 2 instead of expected class 1

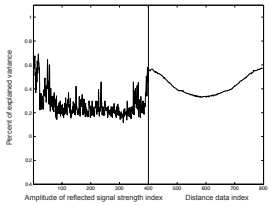

Figure 9: Example of falsely classified scans: identified class 1 instead of expected 2

6 Discussion

With the present architecture, we classify single scans as single entities without considering memory in data. Possible improvements to landmark detection might include bayesian approaches [16], [17] or Canonical Correlation Analysis [18]. However, we have shown in this paper that a simple instantaneous feature extraction and classification scheme is effective for the autonomous identification of most landmarks. These results are similar to other research that has concentrated on the implementation of methods for real-time online identification of landmarks [19], [20], [21] or [22]. We consider the restrictions due to the slow rotational speed of the rotary laser scanner imposed on the travelling velocity of the robot as a special challenge. The introduction of a scanner with a faster rotational speed would provide greater resolution in the z dimension, allowing the effective detection of joint features.

References

[1] K.-U. Scholl, V. Kepplin, K. Berns, and R. Dillmann, "An articulate service robot for autonomous sewer inspection tasks," in *Proceedings of the 1999 IEEE/RSJ International Conference on Intelligent Robots and Systems*, Piscataway, NJ, 1999, vol. 2, pp. 1075–1080, IEEE Press, Kyongju, Korea, October 17–21, 1999.

[2] M. Kolesnik and H. Streich, "Visual orientation and motion control of makro - adaptation to the sewer environment," in *7th International Conference on Simulation of Adaptive Behavior (SAB 2002)*, Berlin, 2002, Springer-Verlag, Edinburg, UK, August 4-9, 2002.

[3] H.-B. Kuntze, D. Schmidt, H. Haffner, and M. Loh, "Karo - a flexible robot for smart sensor-based sewer inspection," in *Proc. 12th International No-Dig conference*, 1995, pp. 367–374, Hamburg, Messe und Congress GmbH.

[4] M. Browne, M. Dorn, R. Ouellette, and S. Shiry, "Wavelet entropy-based feature extraction for crack detection in sewer pipes.," in *6th International Conference on Mechatronics Technology, Kitakyushu, Japan*, 2002.

[5] M. Browne, S. Shiry, M. Dorn, and R. Ouellette, "Visual feature extraction via pca-based parameterization of wavelet density functions," in *International Symposium on Robots and Automation, Toluca, Mexico*, 2002.

[6] J. Hertzberg, T. Christaller, F. Kirchner, U. Licht, and E. Rome, "Sewerobotics," in *From Animals to Animats 5 - Proc. 5th Intl. Conf. on Simulation of Adaptive Behavior (SAB-98)*, R. Pfeifer, B. Blumberg, J.-A. Meyer, and S.W. Wilson, Eds., Boston, USA, 1988, MIT Press.

[7] H.-B. Kuntze, H. Haffner, M. Selig, D. Schmidt, K. Janotta, and M. Loh, "Entwicklung eines flexibel einsetzbaren roboters zur intelligenten sensorbasierten kanalinspektion (karo)," *Dokumentation 4. Internationaler Kongreß Leitungsbau*, pp. 513–528, 1994.

[8] F. Kirchner and J. Hertzberg, "A prototype study of an autonomous robot platform for sewerage system maintenance," *J. Autonomous Robots*, vol. 4, no. 4, pp. 319–331, 1997.

[9] K. Etschberger, *Controller Area Network - Basics, Protocols, Chips and Applications Controller Area Network - Basics, Protocols, Chips and Application*, IXXAT Automation, 2001.

[10] W. Lawrenz, *CAN System Engineering : From Theory to Practical Applications*, Springer, 1997.

[11] M. E. Tipping and C. M. Bishop, "Mixtures of probabilistic principal component analysers," *Neural Computation*, vol. 11, no. 2, pp. 443–482, 1999.

[12] P. R. Gill, W. Murray, and M. H. Wright, *Practical Optimization*, chapter The Levenberg-Marquardt Method, pp. 136–137, Academic Press, London, 1981.

[13] D. M. Bates and D. G. Watts, *Nonlinear Regression and Its Applications*, Wiley, New York, 1988.

[14] C. Goutte and J. Larsen, "Optimal cross- validation split ratio: Experimental investigation," 1998.

[15] C. Goutte, "Note on free lunches and cross-validation," *Neural Computation*, vol. 9, no. 6, pp. 1245–1249, 1997.

[16] D. Fox, W. Burgard, and S. Thrun, "Markov localization for mobile robots in dynamic environments," *Journal of Artificial Intelligence Research*, vol. 11, pp. 391–427, 1999.

[17] L. R. Rabiner, "A tutorial on hidden markov models and selected applications in speech recognition," in *Proceedings of the IEEE, Vol. 77, No. 2*, February 1989.

[18] M. Kuss and T. Graepel, "The geometry of kernel canonical correlation analysis," Tech. Rep. TR-108, Max Planck Institute for Biological Cybernetics, Tübingen, Germany, 2003.

[19] J. Hertzberg and F. Kirchner, "Landmark-based autonomous navigation in sewerage pipes," in *Proc. First Euromicro Workshop on Advanced Mobile Robots (EUROBOT '96)*. 1996, pp. 68–73. Kaiserslautern, IEEE Press.

[20] S. Koenig and R. Simmons, "Unsupervised learning of probabalistic models for robot navigation," in *Proceedings of the IEEE international Conference on Robotics and Automation*, 1996.

[21] T. Belker, M. Hammel, and J. Hertzberg, "Learning to optimize mobile robot navigation based on htn plans," in *Proceedings of ICRA 2003*, Taipeh, Taiwan, September 2003, IEEE.

[22] A. Singhal and C. Brown, "Dynamic bayes net approach to multimodal sensor fusion," 1997.